Available online at www.sciencedirect.com
ScienceDirect
Trans. Nonferrous Met. Soc. China 23(2013) 3611−3620
Transactions of Nonferrous Metals Society of China
www.tnmsc.cn

Influence of heat treatment on microstructures and mechanical properties of gravity cast Mg−4.2Zn−1.5RE−0.7Zr magnesium alloy

Ying-dong WANG[1], Guo-hua WU[1,2], Wen-cai LIU[1], Song PANG[1], Yang ZHANG[1], Wen-jiang DING[1,2]

1. National Engineering Research Center of Light Alloy Net Forming, School of Materials Science and Engineering, Shanghai Jiao Tong University, Shanghai 200240, China;
2. Key State Laboratory of Metal Matrix Composite, School of Materials Science and Engineering, Shanghai Jiao Tong University, Shanghai 200240, China

Received 24 April 2013; accepted 2 August 2013

Abstract: The microstructures and mechanical properties of Mg−4.2Zn−1.5RE−0.7Zr alloy were investigated under different heat treatment conditions. The as-cast alloy consisted of α-Mg phase, T-phase and $Mg_{51}Zn_{20}$ phase. After aging treatment (single-step (325 °C, 10 h) and two-step (325 °C, 4 h)+(175 °C, 14 h)), neither T-phase nor $Mg_{51}Zn_{20}$ phase dissolved into the matrix and the coarsening of α-Mg phase was not significant. When peak-aged at 325 °C for 10 h, dense short rod-like β'_1 phase precipitated in the matrix. Further ageing at 325 °C led to coarsening of β'_1 phase and a decrease in number density. Alloy aged at 325 °C for 10 h achieved the highest yield strength (YS) and ultimate tensile strength (UTS) of 153.9 MPa and 247.0 MPa, which were increased by 48 MPa and 23 MPa from as-cast condition, respectively. While the elongation slightly decreased to 15.6%. Comparatively, the YS and UTS of alloy two-step aged by (325 °C, 4 h)+(175 °C, 14 h) showed little difference from those of single-step aged alloy, but with a lower elongation of 13.4%. In addition, the fracture surfaces of Mg−4.2Zn−1.5RE−0.7Zr alloy under different thermal conditions were mainly characterized by quasi-cleavage feature, but with differences in the details.
Key words: Mg−Zn−RE−Zr alloy; heat treatment; microstructure; mechanical properties

1 Introduction

The extremely low density, superior specific strength and stiffness, excellent damping capacity and good recycling capacity of magnesium alloys make them potential for applications in the automotive, aerospace and electronic industries [1−3]. As one of the precipitation strengthening alloys, the Mg−Zn−Zr alloy system exhibits high strength and good ductility because of the great refinement in microstructure achieved by Zr addition [4]. However, the applications of this alloy system are dramatically restricted by its poor castability, elevated temperature strength and creep resistance [5,6].

It has been reported that the castability and creep resistance of Mg−Zn−Zr alloys can be improved by the addition of RE, which is attributed to the formation of stable MgZnRE ternary eutectic compound in the alloy [7,8]. Previous works have studied the microstructures and phase compositions of Mg−Zn−RE(−Zr) systems, and the results varied with the variety and content of RE elements. WEI et al [9] found that T-phase with c-centered orthorhombic crystal structure and pseudo-binary Mg−Zn phases with small amounts of RE existing in Mg−8Zn−1.5MM (misch metal) alloy. DRITS et al [10] investigated the phase diagram of Mg−Zn−Ce, and detected the presence of binary $Mg_{51}Zn_{20}$ phase and ternary $(Mg_{0.9-0.5}Zn_{0.1-0.5})_{10.1}Ce$ and $Mg_7Zn_{12}Ce$ phases by XRD. LI et al [11] discovered that I-phase with average composition $Mg_{30.02}Zn_{58.94}Er_{11.04}$ (mole fraction, %) and W-phase with average composition $Mg_{37.40}Zn_{38.20}Er_{24.40}$ (mole fraction, %) formed in as-cast Mg−Zn−Er alloy. In addition, the aging hardening behaviors of Mg−Zn−RE(−Zr) alloys have also been investigated. WEI et al [12] concluded that the aging hardening of Mg−Zn−MM(−Zr) alloy aged at 200 °C was mainly caused by a fine dispersion of rod-like β'_1 precipitates, while extensive precipitation of disc-shaped

Foundation item: Project (51275295) supported by the National Natural Science Foundation of China; Project (USCAST2012-15) supported by the Funded Projects of SAST-SJTU Joint Research Centre of Advanced Aerospace Technology, China; Project (20120073120011) supported by the Research Fund for the Doctoral Program of Higher Education of China
Corresponding author: Guo-hua WU; Tel: +86-21-54742630; Fax: +86-21-34202794; E-mail: ghwu@sjtu.edu.cn
DOI: 10.1016/S1003-6326(13)62908-8

β'_2 precipitates coincided with the onset of over-aging. When treated at high temperatures, quasicrystalline phase precipitates (*I*-phase) mainly formed in Mg−Zn−Y alloy instead of β'_1 and β'_2 phases, which has been reported by KIM et al [13].

For Mg−Zn−RE(−Zr) alloys, Mg−4.2Zn−1.5RE−0.7Zr (mass fraction, %) alloy is widely used for aircraft gearbox and generator housings on military helicopters [14,15]. However, the literature available for the microstructure and mechanical properties of Mg−4.2Zn−1.5RE−0.7Zr (mass fraction, %) alloy under different heat treatments remains quite rare. This work is aimed to disclose the relationships between microstructures and mechanical properties under different heat treatment conditions (isothermal single-aging and two-step aging condition) and the optimum heat treatment method for this alloy.

2 Experimental

The material used in this study was Mg−4.2Zn−1.5RE−0.7Zr (mass fraction, %) alloy, which was produced by high-purity elemental Mg (≥99.9%), Zn and Mg−30Zr (mass fraction, %) master alloy, Mg–RE (Ce-rich) mischmetal alloy (the chemical composition is shown in Table 1) in an electric resistance furnace with a mild steel crucible under the mixed atmosphere of CO_2 and SF_6 with the volume ratio of 100:1 and cast in a permanent mould at pouring temperature (730±5) °C. The real chemical composition was determined to be Mg−3.96Zn−1.331RE−0.77Zr (mass fraction, %) by an inductively coupled plasma analyzer (ICP, Perkin Elmer, Plasma−400).

Table 1 Chemical composition of Mg−RE (Ce-rich) mischmetal alloy (mass fraction, %)

Ce	La	Pr	Nd	Si	Fe
14.37	10.84	0.0005	0.0033	0.013	0.050

Ca	Cu	Ni	Mn	Mg
0.0053	0.0011	0.0001	0.014	Balance

Two different heat treatments were investigated in this study. Specimens cut from the cast ingot were isothermally aged at 300, 325, and 350 °C directly in a heat treatment furnace with the protection of SO_2 atmosphere (single-step aging) or first aged at 325 °C and then subsequently aged at 175 °C or 200 °C in an oil-bath (two-step aging). Specimens were cooled down in the air after aging process. The aging response of the alloy was measured by Vickers hardness testing under a load of 49 N with a dwell time of 10 s.

Tensile properties were determined at a initial strain rate of 5×10^{-4} s^{-1} using rectangular specimens with marked dimensions of 15 mm in gauge length, 3.6 mm in width and 2 mm in thickness on Zwick/Roell−20 kN tensile machine at room temperature. Each test condition was repeated at least three times for repeatability and accuracy. Thermal analysis of the alloy was carried out by the differential scanning calorimetry (DSC, STA 449 F3), with a heating rate of 10 K/min under the protection of Ar atmosphere.

The microstructure of the alloy was observed by an optical microscope (OM) and transmission electron microscope (TEM, JEOL−2100) operating at 200 kV. Phase composition was characterized by a scanning electron microscope (SEM, QUANTA FEG 250) and X-ray diffraction using Ni-filtered Cu K_α radiation (XRD). Tensile fracture surface of the studied alloys was also observed by OM and SEM.

3 Results

3.1 Microstructure of as-cast alloy

Figure 1 shows the microstructure of the as-cast Mg−4.2Zn−1.5RE−0.7Zr alloy. As seen from Fig. 1, the microstructure consists of equiaxed α-Mg matrix and eutectic compounds at the grain boundary with inconsecutive reticular structure distribution. The average grain size of α-Mg determined by linear intercept method is (21.38±1.25) μm. Some large particles are also detected at grain interior. They are ZrH_2, Zn_2Zr_3 and some Zr–containing particles which are not unidentified now [16].

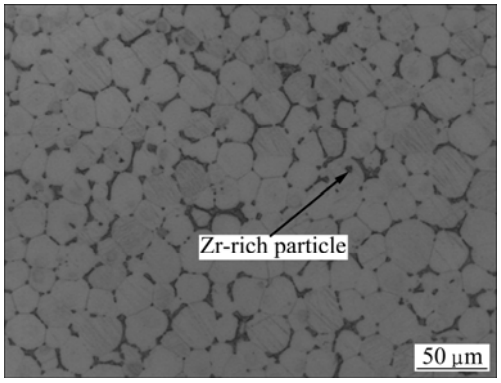

Fig. 1 Microstructure of as-cast Mg−4.2Zn−1.5RE−0.7Zr alloy

The SEM image and corresponding EDS analysis result are presented in Fig. 2 and Table 2, which suggests that the as-cast Mg−4.2Zn−1.5RE−0.7Zr alloy mainly contains two intermetallic phases, i.e. the network-shaped phase along the grain boundary (marked by points *A* and *B*) and triangular-blocky phase at grain boundary triple junction (point *C*), wherein the compositions given by EDS analysis are Mg−24.05Zn−7.32RE, Mg−17.46Zn−6.31RE and Mg−13.77Zn−4.23RE, respectively. This indicates that these eutectic

phases rich in Zn and RE elements should be the ternary *T*-phase, which was identified with c-centered orthorhombic system of a=0.96 nm, b=1.12 nm and c=0.94 nm by WEI et al [9]. Another intermetallic phase formed as a dark gray rim on the existing *T*-phase or a short-bar morphology is designated by points *D* and *E* in Fig. 2, and the EDS analysis detects only a small amount of RE elements in them, about 1.22% and 1.34% (mole fraction), respectively. Apparently, this eutectic phase with a little RE element is different from *T*-phase, and virtually belongs to the binary Mg−Zn phase [9,17]. The phase compositions of the as-cast alloy by XRD analysis are shown in Fig. 3(a). It confirms the existence of *T*-phase and $Mg_{51}Zn_{20}$ phase in the as-cast Mg−4.2Zn−1.5RE−0.7Zr alloy.

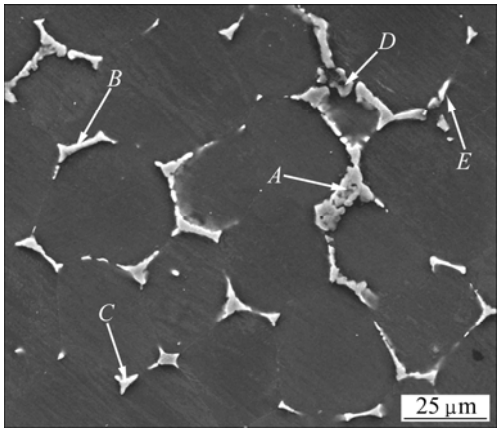

Fig. 2 SEM image and EDS results of as-cast Mg−4.2Zn−1.5RE−0.7Zr alloy

Table 2 EDS results in Fig. 2 for as-cast Mg−4.2Zn−1.5RE−0.7Zr alloy

Eutectic phase	*w*/%			*x*/%		
	Mg	Zn	RE	Mg	Zn	RE
Point *A*	38.22	37.46	24.32	68.63	24.05	7.32
Point *B*	47.84	29.45	22.71	76.23	17.46	6.31
Point *C*	57.15	25.87	16.98	82.00	13.77	4.23
Point *D*	75.46	18.65	5.89	90.48	8.30	1.22
Point *E*	76.52	16.98	6.50	91.14	7.52	1.34

Figure 4 shows the DTA trace of as-cast Mg−4.2Zn−1.5RE−0.7Zr alloy during heating. The DTA curve starts from room temperature to 680 °C with a heating rate of 10 K/min. The first small endothermic peak occurred at about 534.1 °C and the onset temperature was about 525.5 °C, which is in accordance with the melting of the *T*-phase [18]. The second larger peak relating to the melting of the matrix occurred at about 635.5 °C and the onset temperature was about 611.5 °C. However, the DTA trace failed to detect the binary Mg−Zn phases, and it might be due to their small amount in the as-cast alloy.

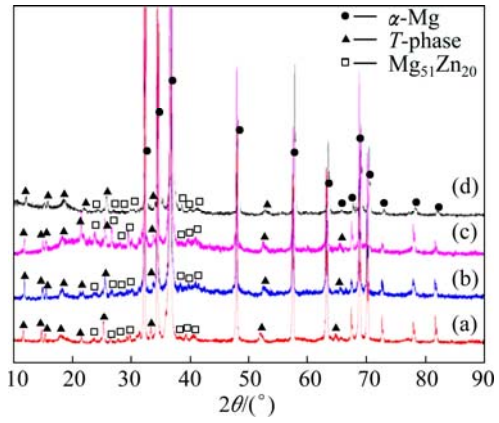

Fig. 3 XRD patterns of Mg−4.2Zn−1.5RE−0.7Zr alloy: (a) As-cast; (b) 325 °C, 10 h; (c) 325 °C, 64 h; (d) (325 °C, 4 h)+(175 °C, 14 h)

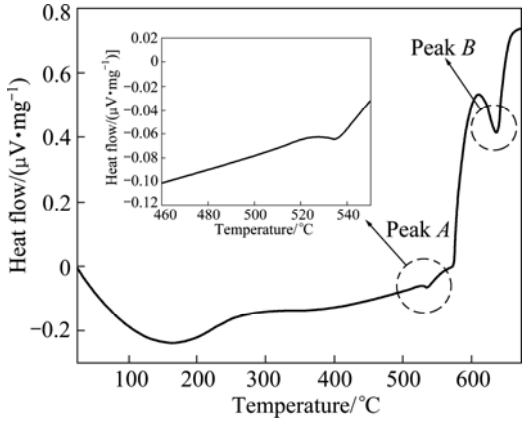

Fig. 4 DTA trace of as-cast Mg−4.2Zn−1.5RE−0.7Zr alloy

3.2 Ageing characteristics

3.2.1 Single-step aging treatment

Figure 5 shows the aging hardening curves of Mg−4.2Zn−1.5RE−0.7Zr alloy isothermally aged at 300, 325 and 350 °C, respectively. The alloy exhibits different ageing hardening behaviors. When aged at 300 °C, the alloy takes 10 h to get the peak hardness of HV67.2, and the increment of the hardness (from as-cast to peak-aged

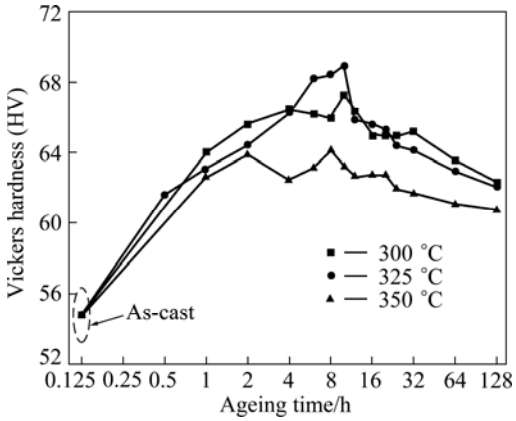

Fig. 5 Isothermal aging hardening response of Mg−4.2Zn−1.5RE−0.7Zr alloy at different temperatures

condition) is close to HV 12.4. While aged at 325 °C, the alloy shows a stronger hardening response with the highest peak hardness of HV 68.9 at 10 h, and the increment of hardness approaches to HV 14.1. Alloy aged at 350 °C exhibits the lowest peak hardness (HV 64.1) but with the shortest time of 8 h to reach the peak hardness, and the increment of hardness is about HV 9.3. Obviously, alloy aged at 325 °C for 10 h reveals the highest peak hardness with the strongest strengthening effect.

Figure 6 shows the microstructure of Mg−4.2Zn−1.5RE−0.7Zr alloy under different isothermal aging conditions. After being aged at 325 °C for 10 h (peak-aged) and 64 h (over-aged), the alloy exhibits the similar microstructure to that of as-cast one (see Fig. 1). The eutectic compounds at grain boundaries almost have no reduction in volume fraction. The average grain size does not change much compared with alloy aged at 325 °C for 10 h ((24.22±1.76) μm), but shows a marked growth to (30.48±0.88) μm when excessively aged for 64 h. The XRD analysis results (see Figs. 3(b) and (c)) and EDS results (see Table 3) show that neither *T*-phase nor $Mg_{51}Zn_{20}$ phase dissolves into the α-Mg matrix after isothermal ageing at 325 °C, indicating that these phases have a relatively good thermal stability. According to Mg−Zn binary diagram [19], $Mg_{51}Zn_{20}$ phase will disappear at 325 °C because the melting point (~340 °C) is approximate to the ageing temperature. Thus, the existence of $Mg_{51}Zn_{20}$ phase after being aged at 325 °C is attributed to the dissolution of a small amount of RE element which increases the melting point [20].

The TEM images and corresponding SAED patterns of precipitates within grains of Mg−4.2Zn− 1.5RE−0.7Zr alloy isothermally aged at 325 °C for 10 h and 128 h are presented in Figs. 7 and 8. As can be seen from Fig. 7(a), dense short rod-shaped precipitates form throughout the α-Mg matrix after being aged at 325 °C for 10 h. The sizes of the precipitates are 3.5−6.7 nm in length and 1.7−2.8 nm in thickness. Figure 8(a) reveals that the precipitates slightly coarsen when aged at 325 °C for 128 h, together with a decrease in number density. The SAED patterns with the electron beam parallel to $[10\bar{1}0]_\alpha$, as shown in Figs. 7(b) and 8(b), indicate that the precipitates under different ageing conditions have the same crystal structure, and they lay on the $(10\bar{1}0)_\alpha$ plane in a parallel way, following $[0001]_\alpha$ direction. The β'_1 phases with hexagonal structure in Mg−Zn−RE alloy [12] usually form as rods with its long axis parallel to the $[0001]_\alpha$ direction. Hence, the precipitates may be β'_1 phases.

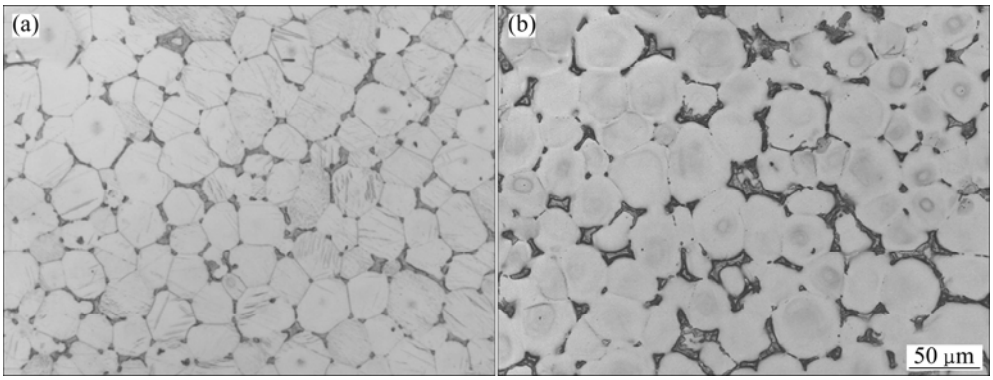

Fig. 6 Optical images of Mg−4.2Zn−1.5RE–0.7Zr alloy under different isothermal ageing conditions: (a) 325 °C, 10 h; (b) 325 °C, 64 h

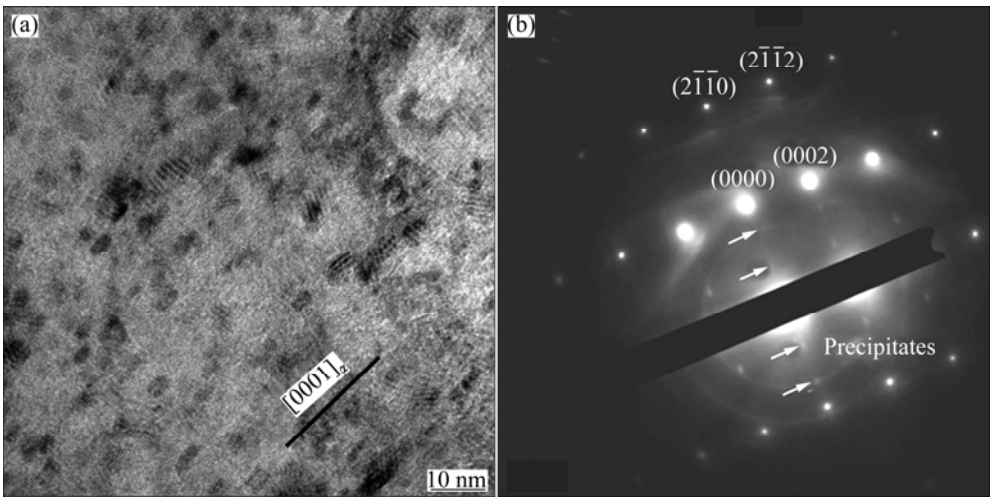

Fig. 7 TEM image (a) and SAED pattern (b) of precipitates after aging at 325 °C for 10 h (along $[10\bar{1}0]_\alpha$ zone axis)

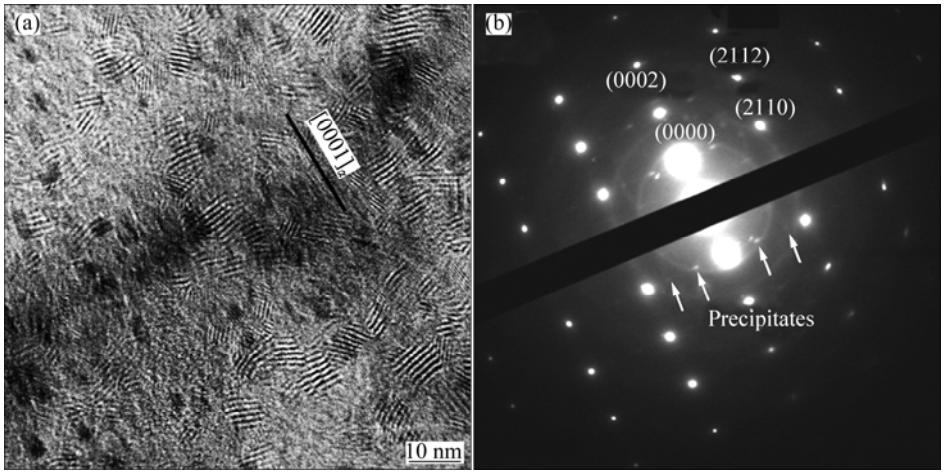

Fig. 8 TEM image (a) and SAED pattern (b) of precipitates after aging at 325 °C for 128 h (along $[10\bar{1}0]_\alpha$ zone axis)

3.2.2 Two-step ageing process

It has been reported that the Mg−Zn−RE alloy could be further hardened by a secondary ageing process at low temperatures [12,14], which may further improve the mechanical properties of the alloy.

Figure 9 shows the effects of ageing time on the hardness of Mg−4.2Zn−1.5RE−0.7Zr alloy during two-step aging process. After being pre-aged at 325 °C for 10 h, the hardness of the alloy first decreases a little and then remains almost unchanged (~HV 67.5) when subjected to the secondary ageing stage at 175 °C, which indicates that this ageing treatment may not improve the mechanical properties. Based on the LAGOWSKI's work [14], the progress of precipitation in Mg−4.2Zn−1.25RE−0.75Zr alloy completed approximately 70% when aged at 330 °C for 2 h. Thus, the precipitation should be almost completed and the precipitates grow after a pre-ageing treatment at 325 °C for 10 h, and the secondary ageing process at temperature of 175 °C will not make any contribution to further precipitating. In this regard, an under-aged condition of 325 °C for 4 h is selected as pre-ageing treatment. As seen in Fig. 9, after being pre-aged at 325 °C for 4 h, the alloy needs 14 h to get the peak hardness (HV67.6) when secondary aged at 175 °C, and the hardness increases by about HV3.7 from pre-ageing condition (HV63.9). The alloy secondary aged at 200 °C for 8 h exhibits a weaker hardening response with a peak hardness of HV66.6, and the increment of hardness from pre-ageing condition is about HV2.7. Apparently, the hardness of the alloy increases when subjected to the secondary ageing stage at 175 °C or 200 °C, and alloy secondary aged at 175 °C exhibits stronger ageing hardening response than 200 °C. This indicates that after a pre-ageing stage of 325 °C for 4 h, the mechanical properties of the alloy could be further improved by the secondary ageing process at low temperature of 175 °C or 200 °C.

Figure 10(c) shows the SEM images of Mg−4.2Zn−1.5RE−0.7Zr alloy after two-step ageing process of (325 °C, 4 h)+(175 °C, 14 h). It indicates that the two-step ageing process makes no change to the eutectic compounds as well as the grain size. Table 3 lists the EDS results of eutectic phase in Fig. 10 for Mg−4.2Zn−1.5RE−0.7Zr alloy. The XRD analysis (Fig. 3(d)) and EDS results (Table 3) suggest that *T*-phase and $Mg_{51}Zn_{20}$ phase still coexist at the grain boundary, which is in accordance with the study of WEI et al [9].

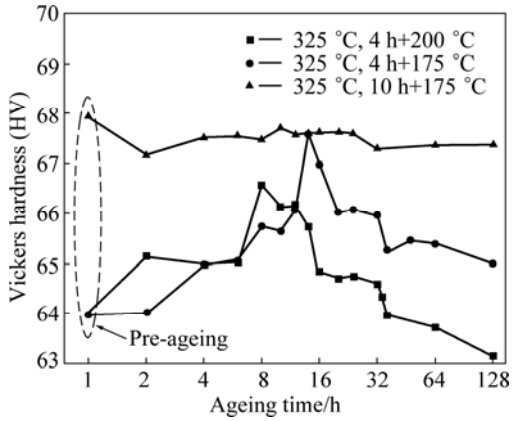

Fig. 9 Two-step ageing hardening response of Mg−4.2Zn−1.5RE−0.7Zr alloy

3.3 Mechanical properties

Tensile properties of Mg−4.2Zn−1.5RE–0.7Zr alloy under different conditions are shown in Fig. 11 and Table 4. As seen from Fig. 11 and Table 4, large improvements of the yield strength (YS) and ultimate tensile strength (UTS) are observed from the as-cast condition to the 325 °C under peak-aged condition, by about 48 MPa and 23 MPa, respectively, while the elongation is slightly reduced by 1.6%. When aged at 325 °C up to 64 h (over-aged), the YS, UTS and elongation drop to 138.6 MPa, 224.2 MPa and 10.9%, respectively. The tensile strength is in accordance with the isothermal ageing hardening curve at 325 °C (see Fig. 5).

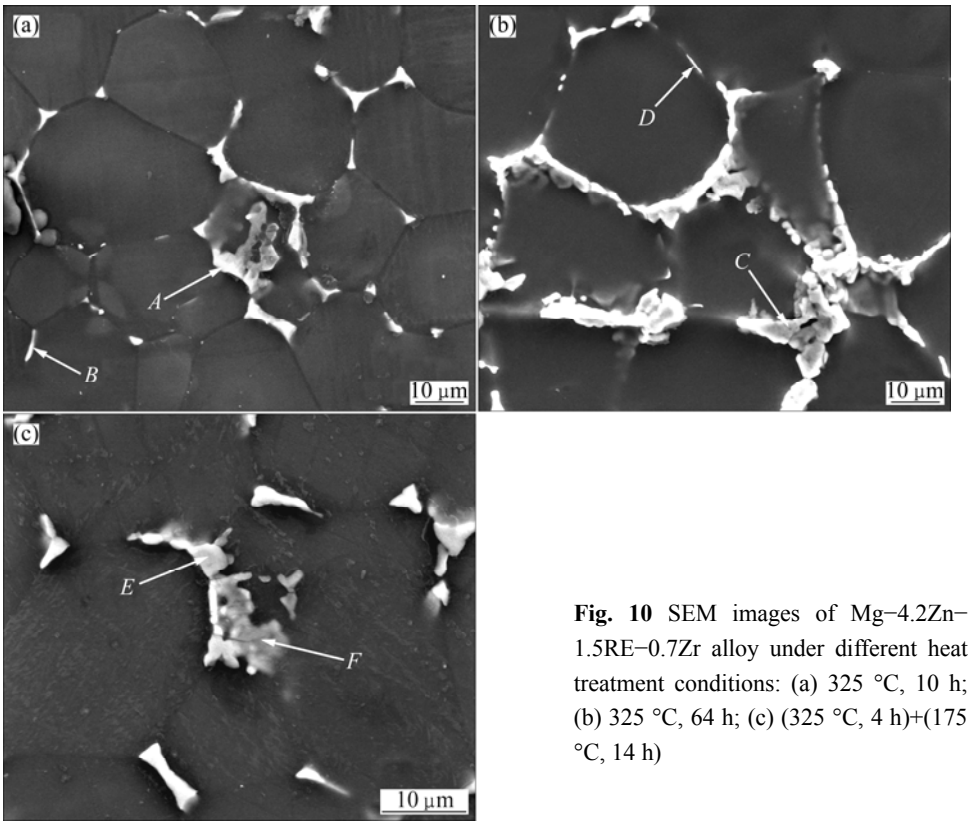

Fig. 10 SEM images of Mg−4.2Zn−1.5RE−0.7Zr alloy under different heat treatment conditions: (a) 325 °C, 10 h; (b) 325 °C, 64 h; (c) (325 °C, 4 h)+(175 °C, 14 h)

Table 3 EDS results of eutectic phase in Fig. 10 for Mg−4.2Zn−1.5RE−0.7Zr alloy

Eutectic phase	*w*/%			*x*/%		
	Mg	Zn	RE	Mg	Zn	RE
Point *A*	48.48	32.13	19.39	75.89	18.83	5.28
Point *B*	82.69	11.57	5.74	93.97	4.89	1.14
Point *C*	49.40	30.49	20.11	76.91	17.65	5.44
Point *D*	86.37	9.95	3.68	95.22	4.08	0.7
Point *E*	56.29	27.14	16.57	81.26	14.57	4.17
Point *F*	75.30	16.34	8.36	90.91	7.34	1.75

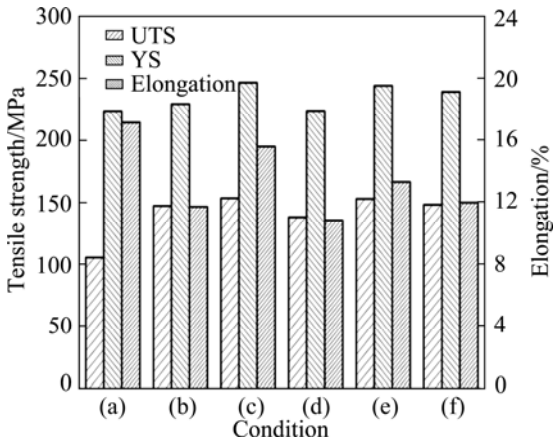

Fig. 11 Tensile properties of Mg−4.2Zn−1.5RE−0.7Zr alloy at room temperature under different conditions: (a) As-cast; (b) 325 °C, 4 h; (c) 325 °C,10 h; (d) 325 °C, 64 h; (e) (325 °C, 4 h)+(175 °C, 14 h); (d) (325 °C, 4 h)+(200 °C, 8 h)

Table 4 Tensile properties of Mg−4.2Zn−1.5RE−0.7Zr alloy under different conditions

Condition	YS/MPa	UTS/MPa	Elongation/%
As-cast	106.0	224.1	17.2
325 °C, 4 h	147.7	229.8	11.8
325 °C, 10 h	153.9	247.0	15.6
325 °C, 64 h	138.6	224.2	10.9
(325 °C, 4 h)+(175 °C, 14 h)	153.4	244.5	13.4
(325 °C, 4 h)+(200 °C, 8 h)	148.8	239.7	12.0

In two-step aging condition, obvious improvements of tensile strengths are firstly achieved by pre-aging stage, with YS and UTS of 147.7 MPa and 229.8 MPa, respectively. While the elongation is greatly reduced from 17.2% in as-cast condition to 11.8% in pre-aged

condition. Further increase of YS and UTS is derived from the secondary ageing stage. Alloy secondary aged at 175 °C for 14 h brings small improvements in YS and UTS, by about 6 MPa and 15 MPa in pre-ageing condition, respectively. The elongation to failure shows a slightly increase to 13.4%.

Apparently, samples in 325 °C peak-aged condition has nearly the same YS and UTS with those in (325 °C, 4 h)+(175 °C, 14 h) condition, but with a higher elongation and shorter aging time. Therefore, ageing at 325 °C for 10 h is taken as the optimal heat treatment condition for Mg−4.2Zn−1.5RE−0.7Zr alloy.

3.4 Fracture behavior

Figure 12 shows the optical microstructures of ruptured samples perpendicular to the fracture surface, which deformed at room temperature during tensile test. Secondary cracks in vicinity of the fracture surfaces are observed. Mg−4.2Zn−1.5RE−0.7Zr alloy shows similar secondary crack location under different thermal conditions. The secondary cracks are all observed along the grain boundaries, mainly inside of the eutectic compounds. This indicates that the secondary cracks are all initiated by the break of eutectics. They propagate along the grain boundaries and merge up with other secondary cracks during the tensile test, leading to final failure.

Figure 13 shows the SEM images of the fracture surfaces of Mg−4.2Zn−1.5RE−0.7Zr alloy under different conditions. As seen from Fig. 13(a), in as-cast alloy, the micro-cracks clearly present in the eutectic compounds, corresponding with the fracture planes cracked along crystal interface of the eutectic structures. This could reflect the intergranular fracture mechanisms. In addition, small cleavage planes are observed, which indicates that after the micro-cracks form in the eutectics, part of them progress across the grains as cleavage fracture. Occasionally some tearing ridges are also observed on the fracture surface, revealing local plastic deformation at grain boundaries without eutectic compounds. Apparently, the fracture mode of as-cast alloy is quasi-cleavage. After being peak-aged at 325 °C, the failure surface is characterized by lots of legible tear ridges, as well as ruptured eutectics and secondary cracks (see Fig. 13(b)). In addition, some coarse dimples occur on the fracture surfaces, indicating local ductile fracture. The fracture surface has a mixed mode of quasi-cleavage and local ductile fracture, corresponding to its high elongation of 15.6%. After being aged at 325 °C for 64 h, the fracture surface shows less and shallower tear ridges and dimples, while large cleavage planes are clearly observed, as seen in Fig. 13(c). This is in accordance with a reduction in elongation to 10.9%. The fracture surface reveals mixed characteristics of quasi-cleavage and cleavage fracture. Figure 13(d) shows the fracture surface in two-step aging condition of (325 °C, 4 h)+(175 °C, 14 h). Local areas reveal the typical characteristic of quasi-cleavage and ductile feature can still be found, which indicates that the fracture surface has also the mixed characteristics. But the fracture

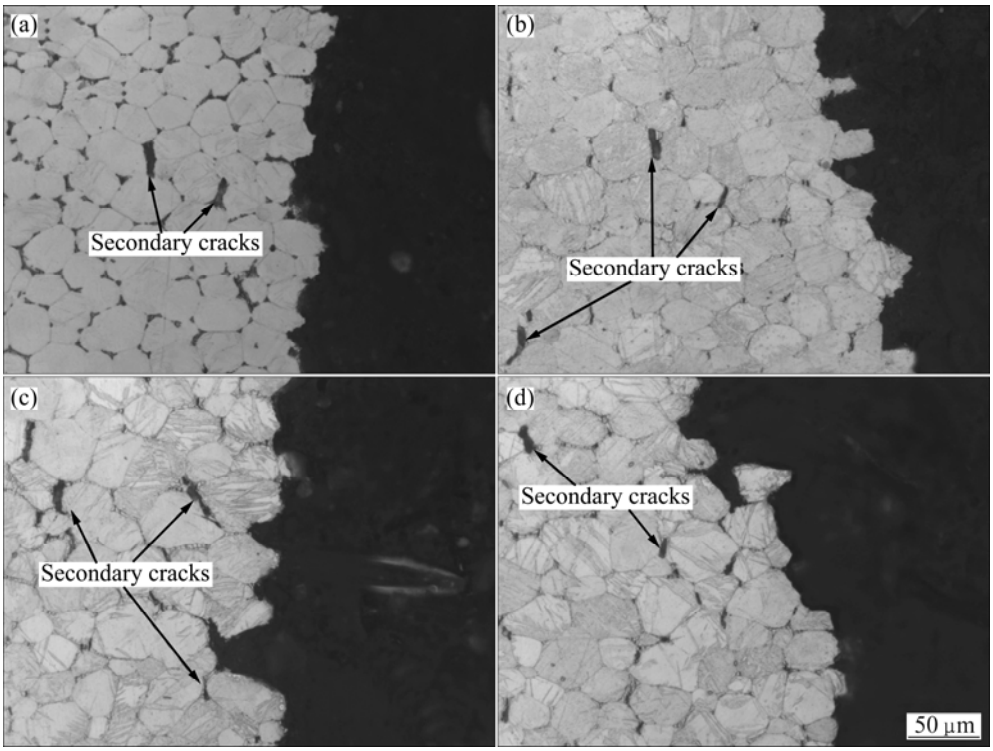

Fig. 12 Optical images of longitudinal section of fracture surfaces of Mg−4.2Zn−1.5RE−0.7Zr alloy under different conditions: (a) As-cast; (b) 325 °C, 10 h; (c) 325 °C, 64 h; (d) (325 °C, 4 h)+(175 °C, 14 h)

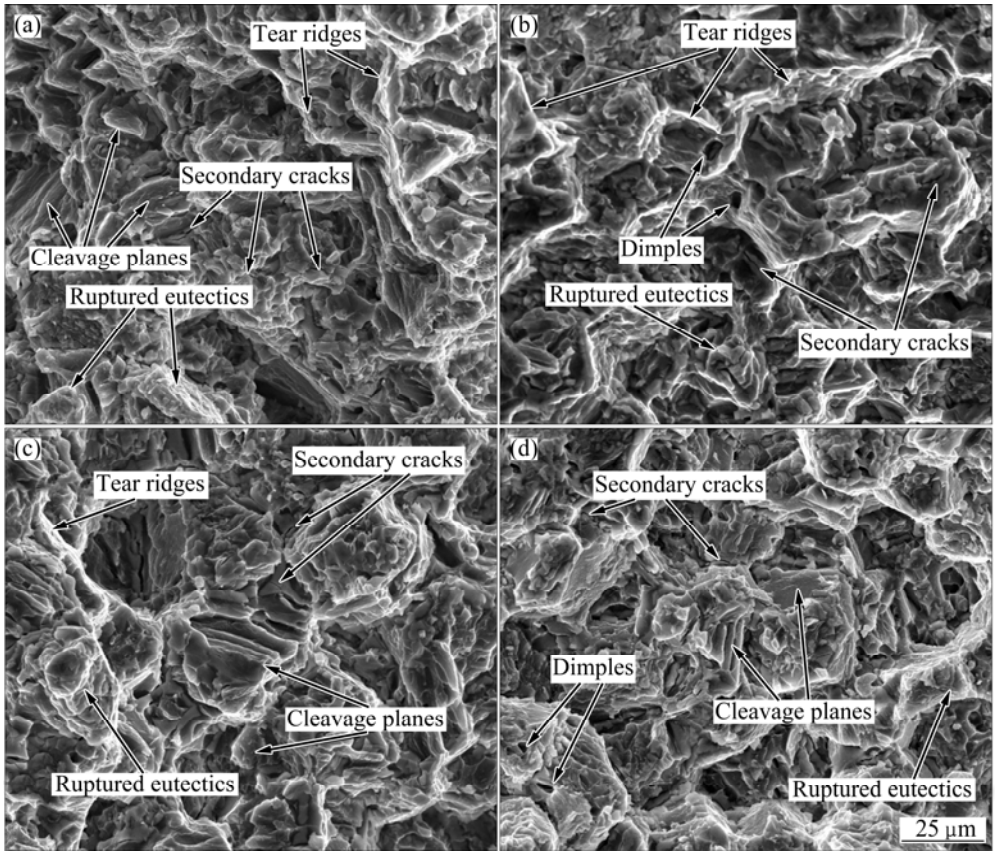

Fig. 13 Typical SEM images of fracture surfaces of Mg−4.2Zn−1.5RE−0.7Zr alloy under different conditions: (a) As-cast; (b) 325 °C, 10 h; (c) 325 °C, 64 h; (d) (325 °C, 4 h)+(175 °C, 14 h)

surface has more small cleavage planes than that aged at 325 °C for 10 h, which results in a slight decrease in ductility.

4 Discussion

In general, four factors contribute to the tensile strength above that of pure Mg. They are secondary phase (eutectic compounds) strengthening, solid solution strengthening, grain boundary strengthening and precipitation strengthening. Compared with the as-cast alloy, it is easy to understand that the mechanical property improvement of the aged alloys is mainly achieved from the precipitation strengthening. In this analysis, the tensile properties (YS and UTS) of the Mg−4.2Zn−1.5RE−0.7Zr alloy aged at 325 °C were discussed with respect to the precipitates and their strengthening mechanism.

After isothermal ageing at 325 °C, the short rod-like precipitates with several nanometers in length form inside the α-Mg grains (see Figs. 7 and 8), and they are supposed to be β'_1 phase. It is well known that the interaction between precipitates and dislocations is an important mechanism for the improvement of mechanical properties of metallic materials. According to the Orowan equation [21], the strengthening effect of shear-resistant precipitates can be assessed in terms of $\Delta\tau$;

$$\Delta\tau = \frac{Gb}{2\pi\lambda\sqrt{1-v}}\ln\left(\frac{d_p}{r_0}\right) \quad (1)$$

where $\Delta\tau$ is the increment in critical resolved shear stress (CRSS) due to dispersion strengthening; G is the shear modulus of the magnesium matrix phase; b is the magnitude of the Burgers vector of the slip dislocations; v is the Poisson ratio; λ is the effective inter-precipitates spacing; d_p is the mean planar diameter of the rods; r_0 is the core radius of dislocations. Equation (1) indicates that the effective planar inter-precipitates space λ plays a quite important role in strengthening the alloy, that is, with the smaller λ, the bypassing of dislocation lines becomes more difficult. TEM images (Figs. 7(a) and 8(a)) indicate that the short rod-like β'_1 precipitates are relatively small and dense when aged at 325 °C for 10 h. Therefore, with closer inter space, the β'_1 precipitates in 325 °C peak-aged condition are more effective in hindering dislocation gliding on basal plane, and the dislocation lines may choose to bypass several closely distributed precipitates at a time [22]. Thus, large CRSS increment is generated by these β'_1 precipitates, resulting

in significant improvements on tensile properties. As can be seen in Table 4, the alloy in 325 °C peak-aged condition has the highest YS and UTS of 153.9 MPa and 247.0 MPa, respectively. Precipitation strengthening contribution to the tensile properties is about 48 MPa in YS and 23 MPa in UTS.

Further ageing at 325 °C leads to coarsening of β'_1 precipitates, together with a decrease in number density (Fig. 8(a)), which deteriorates the precipitation strengthening effect. Moreover, the α-Mg grains grow with the increase of ageing time ((30.48±0.88) μm at 325 °C for 64 h). Therefore, the tensile properties gradually decrease after peak-ageing, and the YS and UTS drop to 138.6 MPa and 224.2 MPa when ageing time reaching 64 h.

5 Conclusions

1) The as-cast Mg−4.2Zn−1.5RE−0.7Zr alloy mainly consists of α-Mg phase, T-phase and $Mg_{51}Zn_{20}$ phase. After ageing treatment (325 °C, 10 h) or (325 °C, 4 h)+(175 °C, 14 h), the eutectic compounds and average grain size are little changed. After being peak-aged at 325 °C for 10 h, a large number of small rod-shaped β'_1 phases precipitate inside the grains. With ageing time prolonging, the precipitates suffer from coarsening and a reduction in number density.

2) After being aged at 325 °C for 10 h, the alloy achieves the highest tensile properties of 153.9 MPa in YS and 247.0 MPa in UTS, which are increased by 48 MPa and 23 MPa from as-cast condition, respectively, while the elongation slightly decreases to 15.6%. The YS and UTS in (325 °C, 4 h)+(175 °C, 14 h) condition have almost the same level with those in (325 °C, 10 h) condition, but with a reduction in elongation to 13.4%. After being aged at 325 °C for 64 h the mechanical properties significantly degrade.

3) The fracture mode of Mg−4.2Zn−1.5RE−0.7Zr alloy under different thermal conditions is mainly quasi-cleavage, but with some distinctions in the details. After being peak-aged at 325 °C and two-step aging condition of (325 °C, 4 h)+(175 °C, 14 h), the fracture surfaces are characterized by some coarse dimples, indicating local ductile fracture. Ageing at 325 °C for 64 h results in large cleavage planes and shallower dimples, which reveals cleavage fracture feature.

References

[1] KAINER K U. Magnesium alloys and technology [M]. New York, NY: Wiley–VCH, 2003: 1−3.

[2] LIU Zhi-jie, WU Guo-hua, LIU Wen-cai, PANG Song, DING Wen-jiang. Effects of heat treatment on microstructures and mechanical properties of sand-cast Mg−4Y−2Nd−1Gd−0.4Zr magnesium alloy [J]. Transactions of Nonferrous Metals Society of China, 2012, 22(7): 1540−1548.

[3] CHEN Xian-hua, HUANG Xiao-wang, PAN Fu-sheng, TANG Ai-tao, WANG Jing-feng, ZHANG Ding-fei. Effects of heat treatment on microstructure and mechanical properties of ZK60 Mg alloy [J]. Transactions of Nonferrous Metals Society of China, 2011, 21(4): 754−760.

[4] LIU Wen-cai, DONG Jie, ZHANG Ping, YAO Zhen-yi, ZHAI Chun-quan, DING Wen-jiang. High cycle fatigue behavior of as-extruded ZK60 magnesium alloy [J]. Material Science and Engineering A, 2009, 44(11): 2916−2924.

[5] ZHOU Tao, XIA Hua, YANG Ming-bo, ZHOU Zhi-ming, CHEN Kang, HU Jian-jun, CHEN Zhen-hua. Investigation on microstructure characterizations and phase compositions of rapidly solidification/powder metallurgy Mg−6wt.%Zn−5wt.% Ce−1.5 wt.% Ca alloy [J]. Journal of Alloys and Compounds, 2011, 509(9): L145−L149.

[6] HUANG Ming-li, LI Hong-xiao, DING Hua, BAO Li, MA Xiao-bin, HAO Shi-ming. Intermetallics and phase relations of Mg–Zn–Ce alloys at 400 °C [J]. Transactions of Nonferrous Metals Society of China, 2012, 22(3): 539−545.

[7] LE Qi-chi, ZHANG Zhi-qiang, SHAO Zhi-wen, CUI Jian-zhong, XIE Yi. Microstructures and mechanical properties of Mg−2%Zn−0.4%RE alloys [J]. Transactions of Nonferrous Metals Society of China, 2010, 20(2): 352−356.

[8] ZHOU Tao, XIA Hua, CHEN Zhen-hua. Effect of Ce on microstructures and mechanical properties of rapidly solidified Mg−Zn alloy [J]. Material Science and Technology, 2011, 27(7): 1198−1205.

[9] WEI L Y, DUNLOP G L, WESTENGEN H. The intergranular microstructure of cast Mg−Zn and Mg−Zn−Rare Earth alloys [J]. Metallurgical and Materials Transactions A, 1995, 26(8): 1947−1955.

[10] DRITS M E, DROZDOVA E I, KOROĹKOVA I G, KINZHIBALO V V, TYYANCHUK A T. Investigation of polythermal sections of the Mg−Zn−Ce system in the Mg–rich region [J]. Russian Metallurgy, 1989, 2: 195−197.

[11] LI Jian-hui, DU Wen-bo, LI Shu-bo, WANG Zhao-hui. Icosahedral quasicrystalline phase in an as-cast Mg−Zn−Er alloy [J]. Rare Metals, 2009, 28(3): 297−301.

[12] WEI L Y, DUNLOP G L, WESTENGEN H. Precipitation hardening of Mg−Zn and Mg−Zn−RE alloys [J]. Metallurgical and Materials Transactions A, 1995, 26(7): 1705−1716.

[13] KIM I J, BAE D H, KIM D H. Precipitates in a Mg−Zn−Y alloy reinforced by an icosahedral quasicrystalline phase [J]. Material Science and Engineering A, 2003, 359(1−2): 313−318.

[14] LAGOWSKI B. Effect of composition and heat treatment on the tensile properties of ZE41 (Mg−4Zn−1RE−0.7Zr) casting alloy [J]. Transactions of the American Foundrymen's Society, 1977, 85: 237−240.

[15] NEIL W C, FORSYTH M, HOWLETT P C, HUTCHINSON C R, HINTON B R W. Corrosion of heat treated magnesium alloy ZE41 [J]. Corrosion Science, 53(10): 3299−3308.

[16] FU Peng-huai, PENG Li-ming, JIANG Hai-yan, ZHAI Chun-quan, GAO Xiang, NIE Jian-feng. Zr-containing precipitates in Mg−3wt%Nd–0.2wt%Zn–0.4wt%Zr alloy during solution treatment at 540 °C [J]. Materials Science Forum, 2007, 546−549: 97−100.

[17] FARZADFAR S A, SANJAN M, JUNG I H, ESSADIQI E, YUE S. Experimental and calculated phases in two as-cast and annealed Mg−Zn−Y alloys [J]. Materials Characterization, 2012, 63: 9−16.

[18] WEI L Y, DUNLOP G L, WESTENGEN H. Solidification behavior and phase constituents of cast Mg−Zn–misch metal alloys [J]. Journal of Materials Science, 1997, 32(12): 3335−3340.

[19] MASSALSKI T B, OKAMOTO H, SUBRAMANIAN P R, KACPRZAK L. Binary alloy phase diagrams [M]. Material Park, Ohio: ASM International, 1996.

[20] HUANG Ming-li, LI Hong-xiao, DING Hua, BAO Li, MA Xiao-bin, HAO Shi-ming. Partial phase relationships of Mg−Zn−Ce system at 350 °C [J]. Transactions of Nonferrous Metals Society of China, 2012, 22(3): 681−685.

[21] NIE Jian-feng. Effects of precipitate shape and orientation on dispersion strengthening in magnesium alloys [J]. Scripta Materialia, 2003, 48(8): 1009−1015.

[22] ZENG Xiao-qing, ZOU Hong-hui, ZHAI Chun-quan, DING Wen-jiang. Research on dynamic precipitation behavior of pre-solution treated Mg−5wt.%Zn−2wt.%Al(−2wt.%Y) alloy during creep [J]. Material Science and Engineering A, 2006, 424(1−2): 40−46.

热处理对铸态 Mg−4.2Zn−1.5RE−0.7Zr 镁合金显微组织和力学性能的影响

王颖东[1]，吴国华[1,2]，刘文才[1]，庞 松[1]，张 扬[1]，丁文江[1,2]

1. 上海交通大学 轻合金精密成型国家工程研究中心，上海 200240；
2. 上海交通大学 金属基复合材料国家重点实验室，上海 200240

摘 要：研究热处理工艺对铸态 Mg−4.2Zn−1.5RE−0.7Zr 镁合金显微组织和力学性能的影响。结果表明：铸态 Mg−4.2Zn−1.5RE−0.7Zr 镁合金的显微组织主要由 α-Mg、T 相和 $Mg_{51}Zn_{20}$ 相组成；单级等温时效(325 °C，10 h)以及双级时效(325 °C，4 h)+(175 °C，14 h)处理均未能使 T 相和 $Mg_{51}Zn_{20}$ 相溶入基体，且晶粒也未明显长大。在 325 °C 下时效 10 h，晶内析出大量短杆状 β'_1 相，延长时效时间将导致 β'_1 相粗化及数量减少。Mg−4.2Zn−1.5RE−0.7Zr 镁合金在 325 °C 下时效 10 h 后具有最高的屈服强度(153.9 MPa)和抗拉强度(247.0 MPa)，相比铸态合金分别增加 48 MPa 和 23 MPa，伸长率降低至 15.6%。Mg−4.2Zn−1.5RE−0.7Zr 合金经双级时效(325 °C，4 h)+(175 °C，14 h)处理后的屈服强度和抗拉强度与单级等温时效处理(325 °C，10 h)的相当，但伸长率有所下降。此外，不同状态下 Mg−Zn−RE−Zr 镁合金的断裂主要表现为准解理断裂，但局部特征有差别。

关键词：Mg−Zn−RE−Zr 合金；热处理；显微组织；力学性能

(Edited by Xiang-qun LI)